



Deposited via The University of York.

White Rose Research Online URL for this paper:

<https://eprints.whiterose.ac.uk/id/eprint/1852/>

Article:

Hirohata, A., Yao, C.C., Hasko, D.G. et al. (1999) Influence of lateral geometry on magnetoresistance and magnetisation reversal in Ni₈₀Fe₂₀ wires. IEEE Transactions on Magnetics. pp. 2865-2867. ISSN: 1941-0069

<https://doi.org/10.1109/20.801007>

Reuse

Items deposited in White Rose Research Online are protected by copyright, with all rights reserved unless indicated otherwise. They may be downloaded and/or printed for private study, or other acts as permitted by national copyright laws. The publisher or other rights holders may allow further reproduction and re-use of the full text version. This is indicated by the licence information on the White Rose Research Online record for the item.

Takedown

If you consider content in White Rose Research Online to be in breach of UK law, please notify us by emailing eprints@whiterose.ac.uk including the URL of the record and the reason for the withdrawal request.

Influence of Lateral Geometry on Magnetoresistance and Magnetisation Reversal in $\text{Ni}_{80}\text{Fe}_{20}$ Wires

C.C. Yao, D.G. Hasko, W.Y. Lee, A. Hirohata, Y.B. Xu, and J.A.C. Bland
Cavendish Laboratory, University of Cambridge, Cambridge CB3 0HE, UK

Abstract — The magnetisation reversal processes and magnetoresistance behaviour in micron-sized $\text{Ni}_{80}\text{Fe}_{20}$ wires with triangular and rectangular modulated width have been studied. The wires were fabricated by electron beam lithography and a lift-off process. A combination of magnetic force microscopy (MFM), magneto-optical Kerr effect (MOKE) and magnetoresistance (MR) measurements shows that the lateral geometry of the wires greatly influences the magnetic and transport properties. The width modulations modify not only the shape-dependent demagnetising fields, but also the current density. The correlation between the lateral geometry, the magnetic and the transport properties is discussed based on MFM, MOKE and MR results.

Index Terms — magnetoresistance, magnetisation reversal, MFM, MOKE

I. INTRODUCTION

As novel magnetic devices are miniaturised, a better understanding of how the lateral geometry affects the magnetic and transport properties of narrow ferromagnetic wires is becoming increasingly important [1-4]. In this work, we have studied the magnetic and transport properties of $\text{Ni}_{80}\text{Fe}_{20}$ wires with periodically triangular and rectangular width modulations. The system of modulated width wires provides an opportunity to explore the relation between the electron transport properties and the modified spin configuration arising from the lateral geometry [5]. It has been found that the magnetisation reversal processes and magnetoresistance (MR) behaviour change significantly in $\text{Ni}_{80}\text{Fe}_{20}$ wires with periodically triangular and rectangular width modulations. The width modulation modifies not only the shape-dependent demagnetising fields, which strongly influence the spin configuration, but also the current density. Unlike in the fixed width wires, the current density is inhomogeneous in the modulated width wires.

In order to study how the lateral geometry affects the magnetisation reversal processes, the magnetic domain configurations in the width modulations have been analysed by magnetic force microscopy (MFM). In addition, transverse and longitudinal microscopic hysteresis loops in the width modulations have also been obtained using magneto-optical effect (MOKE).

II. EXPERIMENTS

The modulated width $\text{Ni}_{80}\text{Fe}_{20}$ wire arrays with triangular and rectangular width modulations were fabricated using electron-beam lithography and a lift-off process. The

Permalloy was electron-beam evaporated onto a GaAs substrate at a pressure 5×10^{-9} mbar and a rate of $2 \text{ \AA}/\text{min}$. The Permalloy wire arrays have a thickness of 300 \AA . The geometry for the triangular and rectangular modulated width wires is shown in Fig. 1. For both modulated width wire arrays, the modulation is repeated over a length of $200 \mu\text{m}$ and the separation between the centres of the wires is $15 \mu\text{m}$. Fig. 2 shows the scanning electron microscopic (SEM) image of the triangular modulated width wire arrays. The image shows that good edge definition has been achieved.

MFM measurements were carried out on a Nanoscope III from Digital Instruments with commercial silicon probes coated with CoCr (Pointprobe magnetic force sensor MESP), at room temperature and in zero field. MOKE measurements were carried out at room temperature in the longitudinal geometry using a stabilised HeNe laser source.

For MR measurements, electrical contacts to the arrays were made using standard optical lithography, metallisation, and lift-off of $25 \text{ nm Cr}/250 \text{ nm Au}$. The voltage probes were separated by $160 \mu\text{m}$. A dc sense current of 1 mA was passed along the wires and the room temperature resistance was recorded automatically using four-terminal method as the in-plane magnetic field was swept. The MR ratio response to magnetic fields H applied along and perpendicular to the wire is defined as $[\text{R}(H)-\text{R}(H=0)]/\text{R}(H=0)$, where $\text{R}(H)$ is the resistance of the sample at a given magnetic field H .

III. RESULTS AND DISCUSSION

Fig. 3 presents the MFM images and domain structures of the triangular and rectangular width modulations in the demagnetising state, which means that the MFM measurements were carried out immediately after the samples were fabricated. It is found that domain walls extend from the corners of the structures. A typical closure domain, seen in micronscale Permalloy squares, is observed in the triangular width modulation, which is in a good agreement with previous work [6]. Our results imply that the number of domains in micronscale wires increases with the complexity of the lateral geometry.

Figs. 4(a) and 4(b) show the MOKE loops for the triangular and rectangular modulations for the fields applied parallel to wire axis, respectively. Both hysteresis loops are rounded, implying that the magnetic easy axis does not purely align to the wire axis direction. It should be noted that for the fixed width wires, the magnetic easy axis direction is the same as the wire axis direction. It is possible to understand this behaviour by considering the shape-dependent demagnetising field [7], which causes magnetically hard behaviour. Since the demagnetising fields are induced by the edge "magnetic charge", it is expected from the geometry of the width modulations that the direction

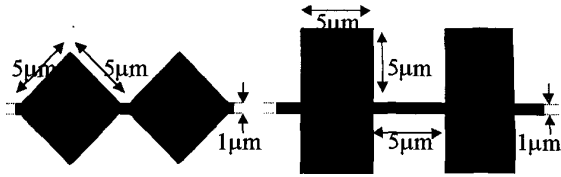


Fig. 1. Schematic of the fabricated triangular and rectangular modulated width wires.

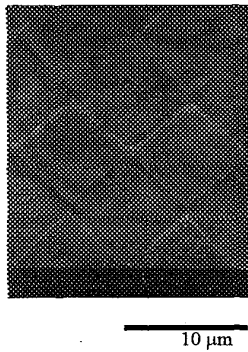


Fig. 2. SEM image of the triangular wire arrays.

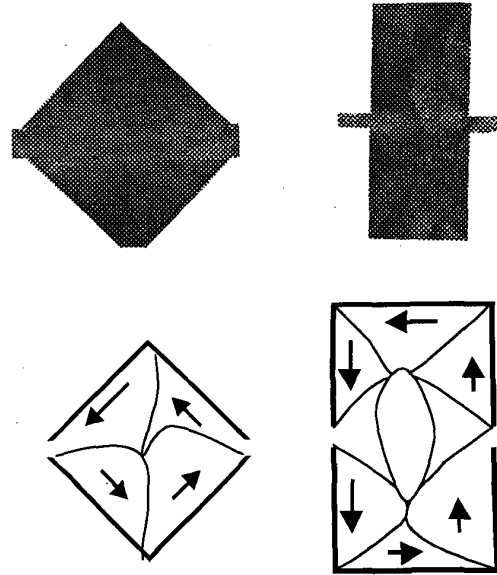


Fig. 3. MFM images and domain structures of the triangular and rectangular width modulation in the demagnetising state.

perpendicular to wire axis is an easy axis direction of this anisotropy. Figs. 4(c) and 4(d) show the MOKE loops for the triangular and rectangular modulations respectively for fields applied perpendicular to the wire axis. We observe that the coercive forces of these hysteresis loops are larger than that of the corresponding hysteresis loops with the fields applied along the wire axis. This confirms that the transverse direction is an easy axis direction.

The results of MR measurements performed on the triangular and rectangular modulated width wires, and the fixed width wires with width equal to 5 μm , respectively, are presented in Fig. 5. For fields applied parallel to the wire axis, the triangular modulated width wires have the highest maximum change in MR ratio (0.34%), compared to the corresponding value for the rectangular modulated width wires (0.22%) and fixed width wires (0.20%). By contrast, for fields applied perpendicular to the wire axis, the maximum change in MR ratio is lowest for the triangular modulated width wires (0.80%), compared to the corresponding value for the rectangular modulated width wires (1.01%) and fixed width wires (1.17%).

Figs 5(a)-5(c) show the MR curves of triangular modulated, rectangular modulated and fixed width wires for the fields applied parallel to wire axis, respectively. Fig. 5(c) shows the typical longitudinal MR curve for fixed width wires [8], in which the sharp resistance minimum corresponds to the switching of the magnetisation in the wires. In Figs. 5(a) and 5(b), an additional transverse MR behaviour and larger longitudinal MR behaviour is observed. Even at the maximum applied field H (600 Oe), the resistance change is not saturated. As the applied field H is

increased from the negative maximum, the resistance clearly increases and drops abruptly before H switches sign. At low positive field, the resistance reaches a minimum and increases, and then decreases again for higher positive fields.

Since MOKE measures the component of the magnetisation along the direction of the applied field, averaged over the focused spot size, this technique is essentially a measurement of $\langle \cos\theta_M \rangle$ when the field is applied along the wire axis, where θ_M is the angle of the magnetisation with respect to the wire axis. The measured MR is mainly due to the anisotropic magnetoresistance (AMR) effect [9-11] which is proportional to $\langle \cos^2\phi \rangle$, where ϕ is the angle between the magnetisation and the current density. In general, $\langle \cos\theta_M \rangle^2$ is not equal to $\langle \cos^2\phi \rangle$, unless all the current density is along the direction of the applied field and θ_M is uniform across the whole sample. However, comparing the MR behaviour in Fig. 5(a) and 5(b) with the corresponding MOKE results in Figs. 4(a) and 4(b), the MR resistance drop before H reverses can be explained by the AMR effect due to the switching of the magnetisation in the width modulations. It is important to note that the measured MOKE signal is dominated by the wide part of the wires and the measured resistance is dominated by the narrow part of the wires because of the width difference. The additional transverse MR behaviour in Figs. 5(a) and 5(b) can be explained by a combination of the AMR effect and the current density distribution in the wide part of the wires. From the hysteresis loops shown in Figs. 4(a) and 4(b), we observe that the magnetisation reversal process is dominated by spin rotation at higher fields, suggesting that the

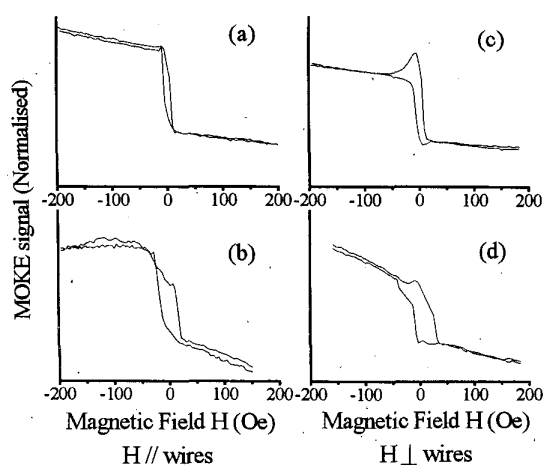


Fig. 4. MOKE hysteresis loops of the (a), (c) triangular modulated width wires, and (b), (d) rectangular modulated width wires for the magnetic field applied along and perpendicular to wire axis, respectively.

transverse MR behaviour is mainly due to the AMR effect in the wide part of the wires where some of the current flow is not parallel to the wire axis.

Figs 5(d)-5(f) show the MR curves of triangular modulated, rectangular modulated and fixed width wires for the fields applied perpendicular to wire axis respectively. In Fig 5(f), a typical negative transverse MR behaviour, nearly reversible and symmetrical with field strength, is observed [8]. This behaviour is consistent with the AMR effect arising from spin rotation dominating the reversal process and suggests that no domain develops across the width of the wires. In Figs. 5(d) and 5(e), two clearly separated peaks in the MR curves are observed, confirming the MOKE results that domain wall motion occurs in the wide part of the wires. By inspection of Figs. 4(c) and 4(d), the peaks in the MR curves correspond to the switching of the magnetisation in the width modulations. This MR behaviour can still be explained in terms of AMR effect with an inhomogeneous current flow in the wide part of the wires.

IV. CONCLUSION

In conclusion, the magnetic and transport properties of micron-sized $\text{Ni}_{80}\text{Fe}_{20}$ wires with triangular and rectangular modulated width have been studied. A combination of magnetic force microscopy (MFM), magneto-optical Kerr effect (MOKE) and magnetoresistance (MR) measurements shows that the lateral geometry of the wires greatly influences the magnetic and transport properties. The correlation between the lateral geometry, the magnetic and transport properties has been discussed based on MFM, MOKE and MR results.

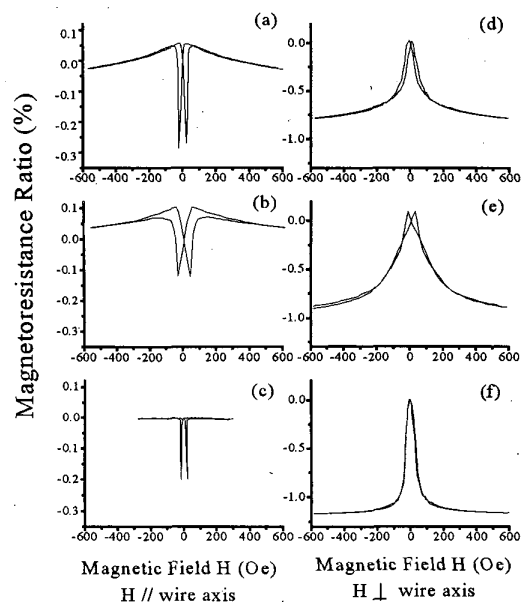


Fig. 5. MR ratio of the (a), (d) triangular modulated width wires, (b), (e) rectangular modulated width wires, and (c), (f) fixed width wires with width equal to $5 \mu\text{m}$ for the magnetic field applied along and perpendicular to wire axis, respectively

ACKNOWLEDGEMENT

The authors would like to thank Prof. H. Ahmed for providing the fabrication facilities for this work. C.C.Y. acknowledges scholarship from the Croucher Foundation.

REFERENCES

- [1] K.J. Krik, J.N. Chapman, and C.D.W. Wilkinson, "Switching fields and magnetostatic interactions of thin film magnetic nanoelements," *Appl. Phys. Lett.* **71**, 539 (1997).
- [2] J.I. Martin et al., "Magnetization reversal in long chains of submicrometric Co dots," *Appl. Phys. Lett.* **72**, 255 (1998).
- [3] K. Hong and N. Giordano, "Approach to mesoscopic magnetic measurements," *Phys. Rev. B* **51**, 9855 (1995).
- [4] C. Shearwood, S.J. Blundell, M.J. Baird, J.A.C. Bland, M. Gester, H. Ahmed and H.P. Hughes, "Magnetoresistance and magnetization in submicron ferromagnetic gratings," *J. Appl. Phys.* **75**, 5249 (1994).
- [5] C.C. Yao, D.G. Hasko, Y.B. Xu, W.Y. Lee, and J.A.C. Bland, "Magnetoresistance in modulated width $\text{Ni}_{80}\text{Fe}_{20}$ wires," *J. Appl. Phys.* **85**, 1689 (1999).
- [6] K. Runge, Y. Nozaki, Y. Otani, and H. Miyajima, "High-resolution observation of magnetization processes in $2 \mu\text{m} \times 2 \mu\text{m} \times 0.04 \mu\text{m}$ permalloy particles," *J. Appl. Phys.* **79**, 5075 (1996).
- [7] R.L. Coren, *J. Appl. Phys.* "Shape demagnetizing effects in Permalloy films," **37**, 230 (1965).
- [8] A.O. Adeyeye, J.A.C. Bland, C. Daboo, D.G. Hasko and H. Ahmed, "Size dependence of the magnetoresistance in submicron FeNi wires," *J. Appl. Phys.* **79**, 6120 (1996).
- [9] T.R. Maguire and R.I. Potter, "Anisotropic magnetoresistance in ferromagnetic 3d alloys," *IEEE Trans. Mag.* **11**, 1018 (1975).
- [10] D.A. Thompson, L.T. Romankiw, and A.F. Mayadas, "Thin film magnetoresistance in memory, storage, and related applications," *IEEE Trans. Mag.* **11**, 1039 (1975).
- [11] P. Ciureanu, "Magnetoresistive Sensors" in *Thin Film Resistive Sensors*, edited by P. Ciureanu and S. Middelhoek (Institute of Physics Publishing, Bristol, 1992), P.253.